



Netrin-3 Suppresses Diabetic Neuropathic Pain by Gating the Intra-epidermal Sprouting of Sensory Axons

Weiping Pan^{1,2} · Xueyin Huang³ · Zikai Yu^{1,2} · Qiongqiong Ding¹ · Liping Xia⁴ · Jianfeng Hua³ · Bokai Gu³ · Qisong Xiong^{1,2} · Hualin Yu^{1,2} · Junbo Wang¹ · Zhenzhong Xu⁴ · Linghui Zeng¹ · Ge Bai^{3,5,6,7} · Huaqing Liu^{1,7}

Received: 29 March 2022 / Accepted: 8 November 2022 / Published online: 1 January 2023
© Center for Excellence in Brain Science and Intelligence Technology, Chinese Academy of Sciences 2022

Abstract Diabetic neuropathic pain (DNP) is the most common disabling complication of diabetes. Emerging evidence has linked the pathogenesis of DNP to the aberrant sprouting of sensory axons into the epidermal area; however, the underlying molecular events remain poorly understood. Here we found that an axon guidance molecule, Netrin-3 (Ntn-3), was expressed in the sensory neurons of mouse dorsal root ganglia (DRGs), and downregulation of Ntn-3 expression was highly correlated with the severity of DNP in a diabetic mouse model. Genetic ablation of Ntn-3 increased the intra-epidermal sprouting of sensory axons and worsened the DNP in diabetic mice. In contrast, the elevation of Ntn-3 levels in DRGs significantly inhibited the intra-epidermal axon sprouting and alleviated DNP in diabetic mice. In conclusion, our studies identified Ntn-3 as an important regulator of DNP pathogenesis by gating the aberrant sprouting of

sensory axons, indicating that Ntn-3 is a potential druggable target for DNP treatment.

Keywords Diabetes · Diabetic neuropathic pain · Netrin-3 · Axon sprouting

Introduction

Diabetic neuropathic pain (DNP) is the most common disabling complication of diabetes, affecting ~30% of diabetic patients [1, 2]. DNP usually begins with increased sensitivity to mechanical and thermal stimuli in the feet [2, 3], then progressively extends to proximal body parts as a continuously burning, tingling, electricity-like, cramping, or aching pain [4, 5]. DNP significantly reduces the quality of life of patients, and there is currently no cure for this disease in the clinic [6–9]. A better understanding of the molecular mechanisms underlying DNP pathogenesis will facilitate the development of more effective treatments for this disease.

In the past decades, several studies have linked DNP to the peripheral nerve damage induced by hyperglycemia and dyslipidemia in diabetes, which may represent one

Weiping Pan, Xueyin Huang, and Zikai Yu contributed equally to this work.

Supplementary Information The online version contains supplementary material available at <https://doi.org/10.1007/s12264-022-01011-8>.

✉ Ge Bai
gebai@zju.edu.cn

✉ Huaqing Liu
liuhq@zucc.edu.cn

¹ Department of Pharmaceutical Sciences, Zhejiang University City College, Hangzhou 310015, China

² College of Pharmaceutical Sciences, Zhejiang University, Hangzhou 310058, China

³ Department of Neurobiology and Department of Neurology of The Second Affiliated Hospital, Zhejiang University School of Medicine, Hangzhou 310058, China

⁴ Department of Anesthesiology and Department of Neurobiology of The First Affiliated Hospital, Zhejiang University School of Medicine, Hangzhou 310058, China

⁵ Liangzhu Laboratory, MOE Frontier Science Center for Brain Science and Brain-machine Integration, State Key Laboratory of Brain-machine Intelligence, Zhejiang University, Hangzhou 311121, China

⁶ NHC and CAMS Key Laboratory of Medical Neurobiology, Zhejiang University, Hangzhou 310058, China

⁷ Institute of Brain and Cognition, Zhejiang University City College School of Medicine, Hangzhou 310015, China

of the earliest pathological changes contributing to the initiation of DNP [1–5]. However, clinical studies have shown that some diabetic patients develop very severe peripheral neuropathy while remaining pain-free [1, 2, 9]. This suggests that, besides nerve damage, other pathological events may also contribute to the development of DNP in diabetes.

Recently, emerging evidence began to reveal that aberrant axon sprouting plays an important role in this process. As a compensatory response to the ongoing axon loss in diabetes, peripheral nerves often exhibit active axon regeneration in patients. However, such peripheral nerve regeneration is insufficient to overcome the ongoing distal axon loss; instead, it often causes the aberrant axon to sprout into epidermal areas, resulting in pain generation. Consistent with this, skin punch biopsies have found a significantly higher density of regenerating nerves in diabetic patients with DNP compared to pain-free patients [10–14]. These findings suggest that the aberrant intra-epidermal axon sprouting may contribute to the pathogenesis of DNP, however, the key signaling molecules implicated in this process remain elusive.

It is known that adult neural regeneration shares molecular and cellular features with neural development [15, 16]. As the first axon guidance molecule to be identified, Netrin-1 (Ntn-1) is well-known for its function in guiding the developing axons to their cellular targets [17–19]. Meanwhile, it has also been found to play important role in regulating neural regeneration and repair [20, 21]. To date, six Ntn family members have been identified in mammals, namely Ntn-1, -3, -4, -5, -G1, and -G2 [22]. In the past decades, most studies were focused on revealing the important roles of Ntn-1, however, the functions of other Ntn family members, such as Ntn-3, remain largely unknown.

Previous studies have shown that Ntn-3 is predominantly expressed in rodent DRGs at the developmental stage [23]. In this study, we found that Ntn-3 sustained its expression in the primary sensory neurons of DRGs until adulthood, and genetic ablation of Ntn-3 in mice did not cause any detectable developmental or behavioral defects. However, in the diabetic mouse model, Ntn-3 deficiency induced a significant increase in the intra-epidermal sprouting of sensory axons, leading to a worse DNP pathogenesis. Conversely, AAV-mediated delivery of Ntn-3 to DRGs significantly inhibited the intra-epidermal axonal sprouting and alleviated DNP in diabetic mice. Above all, our studies reveal that Ntn-3 is a key molecular regulator of DNP pathogenesis by gating the aberrant sprouting of sensory axons. These findings highlight the possibility that Ntn-3-based therapy has the potential for DNP treatment in the future.

Materials and Methods

Mice

The *Ntn-3*-null allele was generated by replacing exon 2 of the mouse *Ntn-3* gene with the coding sequence of the *LacZ* gene and a *neomycin* cassette (KOMP Repository, UC Davis, Davis, CA, USA). Animals with both null alleles were considered to be Ntn-3 KO mice, which were maintained on the C57BL6/J background. Ablation of Ntn-3 expression was confirmed by reverse transcription PCR (RT-PCR) and immunostaining. For RT-PCR analysis of *Ntn-3* expression, the following primers were used (Forward: 5'-CCACGC TTGCCTTGCTTGCTCC-3'; Reverse: 5'-GGTGGCAGT CACAAGCTCTGCAAG-3'). For immunostaining, rabbit anti-Ntn-3 (Invitrogen, 1:1000, Waltham, MA, USA, PA5-62249) was used to detect Ntn-3 expression in mouse L4–L6 DRG samples.

To investigate the effect of Ntn-3 knockout on mouse development, both male and female *Ntn-3* null homozygous (*Ntn-3* KO) mice, Ntn-3 null heterozygous (*Ntn-3* Het) mice, and their wild-type (WT) littermates were examined from birth to 8 weeks old. For behavioral testing and diabetes modeling, 8- to 10-week-old male mice (*Ntn-3* KO or WT littermate controls) were used. Animal procedures and analyses were performed by investigators who were blinded to the animal genotypes and treatment.

All animal studies and experimental procedures were approved by the Animal Care and Use Committee of the animal facility at Zhejiang University. Animals were housed in groups under a 12-h light-dark cycle.

Glucose Tolerance Test

The glucose tolerance test was applied as previously described [24]. Briefly, overnight-fasted mice were intraperitoneally (i.p) injected with 2 g/kg glucose. The blood glucose level was measured at 0 (before injection), 15, 30, 45, 60, and 120 min after injection.

Streptozotocin-induced Diabetic Mouse Model

Diabetes was induced in mice by 2 consecutive days of STZ (Sigma, Burlington, MA, USA) administration, which is the most stable regime to induce diabetic polyneuropathy [25]. All mice were injected with STZ (100 mg/kg, i.p) or an equivalent volume of vehicle (Veh, citrate buffer, pH 4.5) on two consecutive days. The cumulative dose of STZ was 200 mg/kg. The blood glucose concentration was monitored every week; >15 mmol/L for two consecutive weeks was considered to be diabetes. Animals with blood

glucose concentrations <15 mmol/L were excluded from the experiments. Body weight was monitored weekly after STZ administration.

Evaluating the Anxiety Levels and Motor Functions

The sensory function test depends on the reliable responses of testing animals, therefore the influence of animals' anxiety or potential motor deficits needs to be excluded. Therefore, *Ntn-3* KO animals were pre-evaluated for anxiety levels and motor functions. The open-field test was used to evaluate the locomotor activity and anxiety-like behaviors. The fear conditioning test was used to evaluate fear memory [26, 27]. Motor function and motor-sensory coordination were tested by using rotarod, grip strength, and horizontal ladder tests as previously described [28, 29].

Mechanical Allodynia

Mechanical allodynia was evaluated by the von Frey filament test. Briefly, mice were placed separately in a plastic cage on wire mesh and acclimatized for at least 30 min each day for 2 days before testing. For testing, a calibrated von Frey filament was applied to the plantar surface of the hind paw, and the 50% paw withdrawal threshold was calculated by the up-and-down method [30].

Cold Allodynia

Cold allodynia was tested by applying a drop of acetone to the ventral surface of the hind paw as previously described [31]. The response to acetone was scored from 0 to 5 according to the following scale: 0 = no response, 1 = brief lift, sniff, flick, or startle; 2 = jumping and paw shaking; 3 = multiple lifts and paw licks; 4 = prolonged paw lifting, licking, shaking or jumping; 5 = paw guarding. Mice were tested three times on each paw with an interval of 20 min between tests. The average of three scores of each animal was used in the analysis.

Thermal Hyperalgesia

Thermal hyperalgesia was tested in mice with a plantar test device (Plantar Test Serial N, Ugo Basile, Gemonio, VA, Italy). The latency of paw withdrawal from a radiant heat stimulus was recorded. Mice were acclimated to the testing environment each day for 2 days before testing. For testing, the mice were placed on a glass platform under an acrylic box for at least 30 min until they settled. Paw withdrawal latency in response to the heat stimulus was measured three times on each hind paw at 10-min interstimulus intervals. The average of three latencies was used for analysis [32].

Dil Injection and Retrograde Labeling

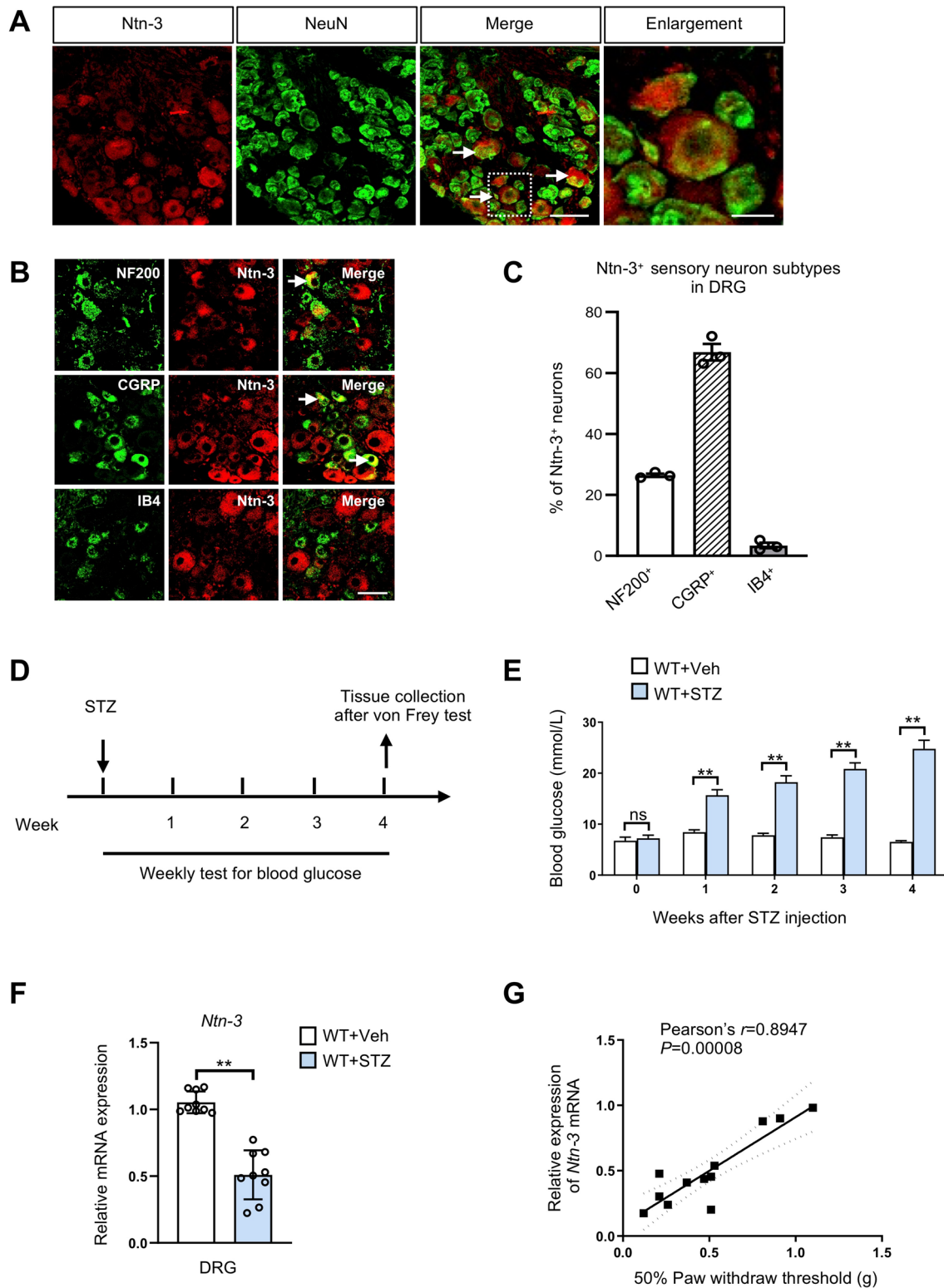
Sensory neurons with epidermal innervation were retrogradely labeled by 1,1'-dioctadecyl-3,3,3',3'-tetramethylindocarbocyanine perchlorate (Dil) injection [33]. Briefly, 1 μ L Dil (5 mg/mL in DMSO, MCE, Monmouth Junction, NJ, USA) was applied *via* a Hamilton syringe at multiple sites on the skin of the footpad. Ten days after the injections, the L4–L6 spinal cord and corresponding DRGs were collected for immunohistochemistry.

Immunofluorescent Staining

Deeply-anesthetized mice were perfused with 4% paraformaldehyde. The sciatic nerve, hind paw plantar skin, L4–L6 spinal cord, and DRGs were collected for cryostat sectioning at 20 μ m. Tissue sections were incubated overnight with the primary antibodies: rabbit anti-Ntn-3 (1:1000, Invitrogen, Waltham, MA, USA, PA5-62249); rabbit anti-neurofilament 200 (NF200, 1:1000, Millipore, Burlington, MA, USA, ab1991); rabbit anti-growth associated protein 43 (GAP-43, 1:1000, Millipore, ab5220); rabbit anti-ionized Ca²⁺-binding adapter molecule 1 (Iba1, 1:1000, Wako, Richmond, VA, USA, 019-19741); mouse anti-glial fibrillary acidic protein (GFAP, 1:200, Santa Cruz, Dallas, TX, USA, sc-33673); mouse anti-protein gene product 9.5 (PGP9.5, 1:1000, Abcam, Cambridge, UK, ab8189); mouse anti-calcitonin gene-related peptide (CGRP, 1:1000, Abcam, ab81887); GS-isolectin B4 (IB4) Alexa Fluor™ 488 (1:1000, Thermofisher, Waltham, MA, USA, I21411); and rabbit anti-V5 (1:1000, Cell Signaling Technology, Danvers, MA, USA, 13202). Sections were then incubated with secondary antibodies conjugated with Alexa Fluor 488 or 546 (1:1000, Invitrogen, A11008, or A11029) for 1 h at room temperature. Images were acquired by confocal microscopy (Olympus FV3000, Shinjuku, Tokyo, Japan) and analyzed using ImageJ software (National Institutes of Health, Bethesda, MD, USA).

Quantification of Epidermal Axons

PGP9.5-labeled intra-epidermal nerve fiber density was assessed and is presented as the mean number of fibers crossing the dermal/epidermal junction per linear millimeter of the epidermis as previously described [34, 35]. The abundance of GAP-43⁺ axon sprouting was quantified and is presented as the GAP-43⁺ fluorescence intensity per $2 \times 10^4 \mu\text{m}^2$ of the epidermis (arbitrary units, a.u.). Five adjacent fields from six tissue sections per mouse were used for quantification.



Quantitative Real-time PCR

Mouse sciatic nerves, L4–L6 DRGs, and spinal cords were collected for qPCR analysis as previously described [36]. Briefly, their total RNAs were extracted using TRIzol

reagent (ThermoFisher, Waltham, MA, USA, 15596018) and RNeasy mini column (Qiagen, Hilden, Germany, 217004). The cDNA was synthesized by using HiScript II Q Select RT SuperMix (Vazyme Biotech, Nanjing, Jiangsu, China, R232-01). Gene expression was determined by quantitative

Fig. 1 Ntn-3 is expressed in DRG sensory neurons and its expression is inversely correlated with the severity of DNP. **A** Immunostaining of Ntn-3 colocalized with NeuN (arrows) in the DRGs of adult WT mice. Scale bar, 50 μ m. The boxed region of the merged images is enlarged on the right. Scale bar, 15 μ m. **B** Co-immunostaining of Ntn-3 and neuronal subtype markers in mouse DRGs. Ntn-3 is expressed in NF200⁺ and CGRP⁺ neurons (arrows), but rarely in IB4⁺ neurons. Scale bar, 50 μ m. **C** The ratio of neuronal subtypes in total Ntn-3⁺ neurons. $n = 3$ mice. **D** Schematic of the experimental design. **E** Weekly blood glucose tests show that hyperglycemia is induced by STZ administration in mice. $**P < 0.01$; ns, no significant difference by Student's *t*-test. $n = 9$ mice per group. **F** qPCR analysis show that *Ntn-3* expression is downregulated in the DRGs of DNP mice. $**P < 0.01$. ns, no significant difference by Student's *t*-test. $n = 9$ mice per group. **G** *Ntn-3* expression in DRGs is significantly correlated with the mechanical pain threshold in diabetic mice at 4 weeks after STZ administration. $n = 12$ mice.

PCR (qPCR) with GAPDH as the internal control. The information on primer pairs is listed in supplemental Table S1.

Transmission Electron Microscopy (TEM)

Isolated sciatic nerves were placed in 0.1 mol/L phosphate buffer containing 2.5% glutaraldehyde, osmicated, dehydrated, and embedded with Araldite resin (SPI Supplies Division Structure Probe, West Chester, PA, USA, 02828-AF). Sciatic nerves were cut at 100 nm on an automated microtome (Leica, Wetzlar, Germany, RM2065). Tissue sections were stained with uranyl acetate and imaged in a TECNAI 10 projection electron microscope [37]. Axon degeneration was quantified by morphological hallmarks. The density of myelinated fibers and the total transverse area of unmyelinated axons in each frame area ($3.5 \times 3.5 \mu\text{m}^2$) were quantified [36]. The axon g-ratio was analyzed by ImageJ as previously described [38].

Elevation of *Ntn-3* Expression in Mouse DRGs

For AAV-*Ntn-3* preparations, *Ntn-3* cDNA was fused with a V5 tag, which was inserted into the AAV2/9 vectors with its expression under the control of the CMV promoter (BrainVTA Wuhan Co., Ltd, Wuhan, Hubei, China). The viral titer was 1×10^{13} viral genomes per milliliter (vg/mL). AAV-*Ntn-3* or AAV-*GFP* (control) was delivered by intrathecal injection (i.t). Briefly, the spinal cord was first punctured with a 30-G needle between L5 and L6; then 10 μ L AAV was injected into the cerebrospinal fluid [39, 40]. The expression of AAV-*Ntn-3* was further determined by qPCR.

Gene Expression Omnibus (GEO) Dataset Analysis

RNA-sequencing (RNA-seq) data of sural nerves in diabetic patients was from a published database, GSE148059 (NCBI Gene Expression Omnibus, Accession ID: GSE 148059, <http://www.ilincs.org/apps/greinj/>) [41]. Sural nerve samples

from type 2 diabetic patients had been monitored for >52 weeks. Based on the changes in myelinated fiber density (Δ MFD%), subjects had been divided into regenerator and intermediator groups according to different regenerative statuses as previously described: the mean Δ MFD% \pm SD was 35.6 ± 17.4 for the regenerator group, and 4.8 ± 12.1 for intermediator group [42]. Each group contained at least 14 individual patient samples. The expression of Ntn family members was analyzed for each patient group.

Statistical Analysis

All data and graphs were analyzed using GraphPad Prism 7.0 software (MacKiev). Unpaired Student's *t*-tests were used for analysis between two groups. When comparing the effect of two factors on multiple groups, two-way ANOVA followed by Tukey's *post hoc* test was used. $P < 0.05$ was considered significant, and the *P*-value for each experiment is given in the figure legends. The correlation was analyzed by Pearson's correlation coefficient. Data are presented as the mean \pm SEM. All data were analyzed by investigators blinded to experimental groups.

Results

Ntn-3 is Expressed in DRG Sensory Neurons

Previous studies have found that Ntn-3 is predominantly expressed in the DRGs at the embryonic stage [23], therefore we wondered whether Ntn-3 can sustain its expression until adulthood. By immunohistochemistry using the Ntn-3 antibody, we found that Ntn-3 was mainly expressed in NeuN⁺ DRG sensory neurons with its expression predominantly in the CGRP⁺ neuronal subtype but less in the NF200⁺ and IB4⁺ neuronal subtypes (Fig. 1A–C). Besides the DRGs, Ntn-3 expression was also detected in other neural tissues including the brain, spinal cord, and nerve (Fig. S1).

To investigate the function of Ntn-3, *Ntn-3* KO mice were generated by replacing exon-2 with lacZ and Neo cassettes in the *Ntn-3* gene loci. Depletion of Ntn-3 expression was confirmed by RT-PCR and immunostaining with Ntn-3 antibodies (Fig. S2A, B). First, we found that the birth ratio of *Ntn-3* Het/Het breeding was consistent with Mendel's law (Fig. S2C), suggesting the normal viability of *Ntn-3* KO mice at birth. Next, *Ntn-3* KO mice had body weights and behavioral functions similar to their WT littermates (Fig. S2D–O). For example, fear conditioning and the elevated plus-maze test showed that *Ntn-3* KO mice exhibited normal anxiety-like behaviors similar to their WT controls (Fig. S2E–G); open-field and rotarod tests showed that Ntn-3 depletion did not affect the spontaneous motor activity or motor-sensory coordination (Fig. S2I–K); the sensory function of *Ntn-3* KO

mice was also comparable to their WT controls, as indicated by measurements of their mechanical and cold allodynia as well as thermal hyperalgesia (Fig. S2M–O). Altogether, these data suggested that Ntn-3 is dispensable for embryonic development and physiological functions in mice.

Downregulation of Ntn-3 Expression is Highly Correlated to the Severity of Diabetic Neuropathic Pain

Next, we wondered whether Ntn-3 plays a role in pathological conditions such as DNP. To investigate this, STZ was used to induce diabetes in mice (Fig. 1D), and the blood glucose level was monitored as an indicator of hyperglycemic progression. We found that the blood glucose levels rose from week 1 after STZ, then gradually increased in the following weeks (Fig. 1E). In week 4 after STZ, the development of DNP in each animal was evaluated by measuring the mechanical allodynia using the von Frey test. Animals with mechanical pain thresholds that dropped to <30% of the baseline level were considered to experience severe mechanical allodynia. At this stage, the expression of Ntn-3 was also assessed in DRGs by qPCR analysis. We found that Ntn-3 expression was significantly decreased in diabetic mice with severe mechanical allodynia compared to their vehicle-treated littermates (Fig. 1F). Among the diabetic animals, there was a distinct correlation between the decrease of Ntn-3 expression and the severity of mechanical allodynia (Pearson's correlation coefficient: $r = 0.8947$, $P < 0.00001$; Fig. 1G). However, the expression of other Ntn members, such as Ntn-1 and Ntn-4, was less correlated with the severity of mechanical allodynia (Fig. S3A, B). Altogether, these data link Ntn-3 to the pathogenesis of DNP in diabetes.

Ntn-3 Depletion Aggravates the Neuropathic Pain in Diabetic Mice

To verify the involvement of Ntn-3 in DNP pathogenesis, we assessed neuropathic pain in diabetic *Ntn-3* KO mice. First, we found that *Ntn-3* KO mice displayed a normal glucose metabolism in the glucose challenge test, which was comparable to WT mice (Fig. 2A). We also found that *Ntn-3* KO mice exhibited significantly increased concentrations of blood glucose and decreased body weights, similar to their WT littermates (Fig. 2B, C). These results suggested that Ntn-3 depletion has no significant effect on the progression of STZ-induced diabetes.

During this period, the development of DNP was monitored in diabetic WT and *Ntn-3* KO mice by the von Frey test every week. We found that animals began to show signs of mechanical allodynia 2 weeks after STZ administration. At this stage, no significant difference was found between diabetic WT and *Ntn-3* KO mice. Starting from week 3 after STZ, the mechanical allodynia of diabetic *Ntn-3* KO

mice began to get worse than their diabetic WT littermates (Fig. 2D). In week 4 after STZ, the diabetic *Ntn-3* KO mice also developed more severe cold allodynia than diabetic WT mice in the acetone test (Fig. 2E). However, their thermal pain levels remained comparable to the diabetic WT mice in the thermal hyperalgesia test (Fig. 2F). These data suggested that Ntn-3 deficiency worsens the mechanical and cold allodynia in diabetic mice.

Ntn-3 Deficiency does not Aggravate Peripheral Nerve Damage in Diabetic Mice

Since previous studies have linked DNP pathogenesis to peripheral nerve damage in diabetes [43], we wondered whether Ntn-3 depletion influences this pathological process. To test this idea, we first assessed the proximal nerve damage by collecting sciatic nerves from diabetic WT and *Ntn-3* KO mice. Transmission electron microscopy (TEM) revealed remarkable signs of axon degeneration and demyelination in sciatic nerves from STZ-induced diabetic WT mice compared to vehicle controls (Fig. 3A), which was confirmed by the analysis of their axon degeneration ratio (an indicator of axon degeneration) and *g*-ratio (an indicator of demyelination) (Fig. 3B, C). However, at this stage, we found no changes in the density of myelinated axons and coverage area of nonmyelinated axons in STZ-induced diabetic mice (Fig. S4A, B), indicating that there was no axon loss despite marked axon damage. Moreover, we found no significant difference between diabetic *Ntn-3* KO mice and their diabetic WT littermates on all of the indicators of axon pathology (Figs 3A–C and S4A, B). These analyses of pathology suggested that Ntn-3 depletion does not affect the progress of axon damage in sciatic nerves in week 4 after STZ administration. Since diabetic neuropathy is often initiated in distal nerves, we then examined the distal nerve damage by collecting skin samples from the hind paws of diabetic WT and *Ntn-3* KO mice. The density of intra-epidermal nerve fibers was analyzed by immunostaining using PGP9.5 antibodies. In week 4 after STZ, we found a significant reduction of intra-epidermal nerve fiber density in both diabetic WT and *Ntn-3* KO mice, while there was no difference between them (Fig. 3D). Taken together, these data suggested that peripheral nerve damage is not the major contributor to the worsened DNP in *Ntn-3* KO mice, at least in the early stage of STZ-induced diabetic neuropathy.

Ntn-3 Deficiency does not Affect DNP-associated Neuroinflammation

Similar to other types of neuropathic pain, neuroinflammation also contributes to the pathogenesis of DNP [5, 44]. Therefore, the neuroinflammation-associated gliosis was first determined in the spinal cords of diabetic WT and *Ntn-3*

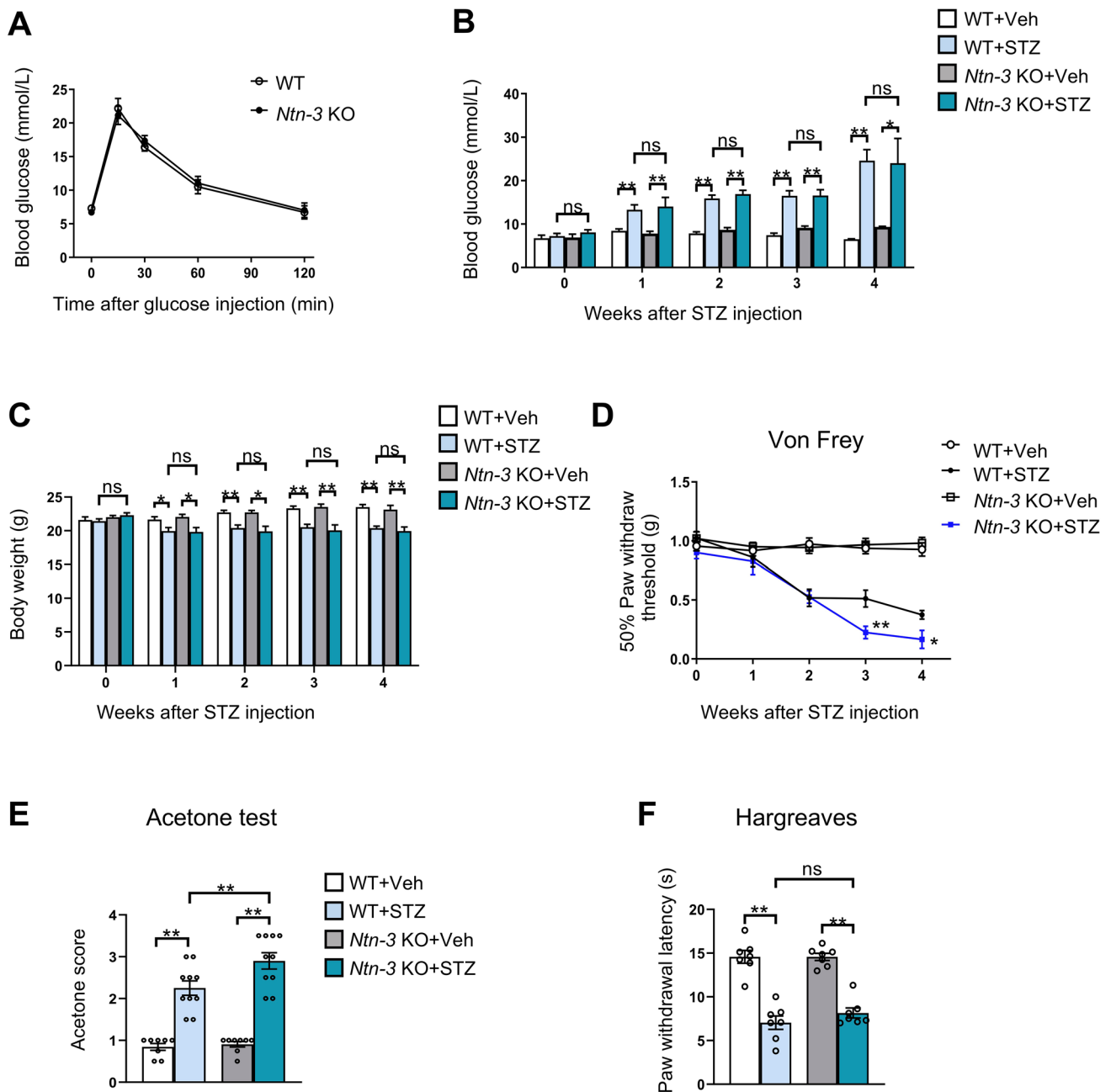


Fig. 2 *Ntn-3* deficiency triggers hypersensitivity of mechanical and cold allodynia in diabetic mice. **A** *Ntn-3* KO mice perform normally in the glucose tolerance test. $n = 8$ mice per group. **B**, **C** Weekly blood glucose tests and body weight measurements indicate that *Ntn-3* KO mice respond to STZ-induced hyperglycemia in a similar manner to that of WT littermates. $*P < 0.05$; $**P < 0.01$; ns, no significant difference by two-way ANOVA. $n = 8$ –12 mice per group. **D** The mechanical pain threshold is significantly decreased in *Ntn-3*

KO mice compared with WT littermates during DNP progression. $*P < 0.05$; $**P < 0.01$ compared with the WT+STZ group by two-way ANOVA. $n = 11$ mice per group. **E** Increased cold allodynia in *Ntn-3* KO mice compared with WT littermates at week 4 after STZ administration. $**P < 0.01$ by two-way ANOVA. $n = 8$ –10 mice per group. **F** No significant differences are found in thermal hyperalgesia between diabetic *Ntn-3* KO and WT mice. $n = 7$ mice per group. $**P < 0.01$. ns, no significant difference by two-way ANOVA.

KO mice by immunohistochemistry. We found significant activation of astrogliosis (GFAP⁺) and microgliosis (Iba1⁺) in both STZ-induced diabetic WT and *Ntn-3* KO mice compared to their vehicle controls, while there was no difference between WT and *Ntn-3* KO mice regardless of STZ or

vehicle administration (Fig. S4C, D). Next, we examined the expression of the main cytokines responsible for neuropathic pain, interleukin-1 (IL-1), tumor growth factor-beta (TGF- β), and nerve growth factor (NGF), in diabetic animals. Both STZ-treated WT and *Ntn-3* KO mice exhibited a

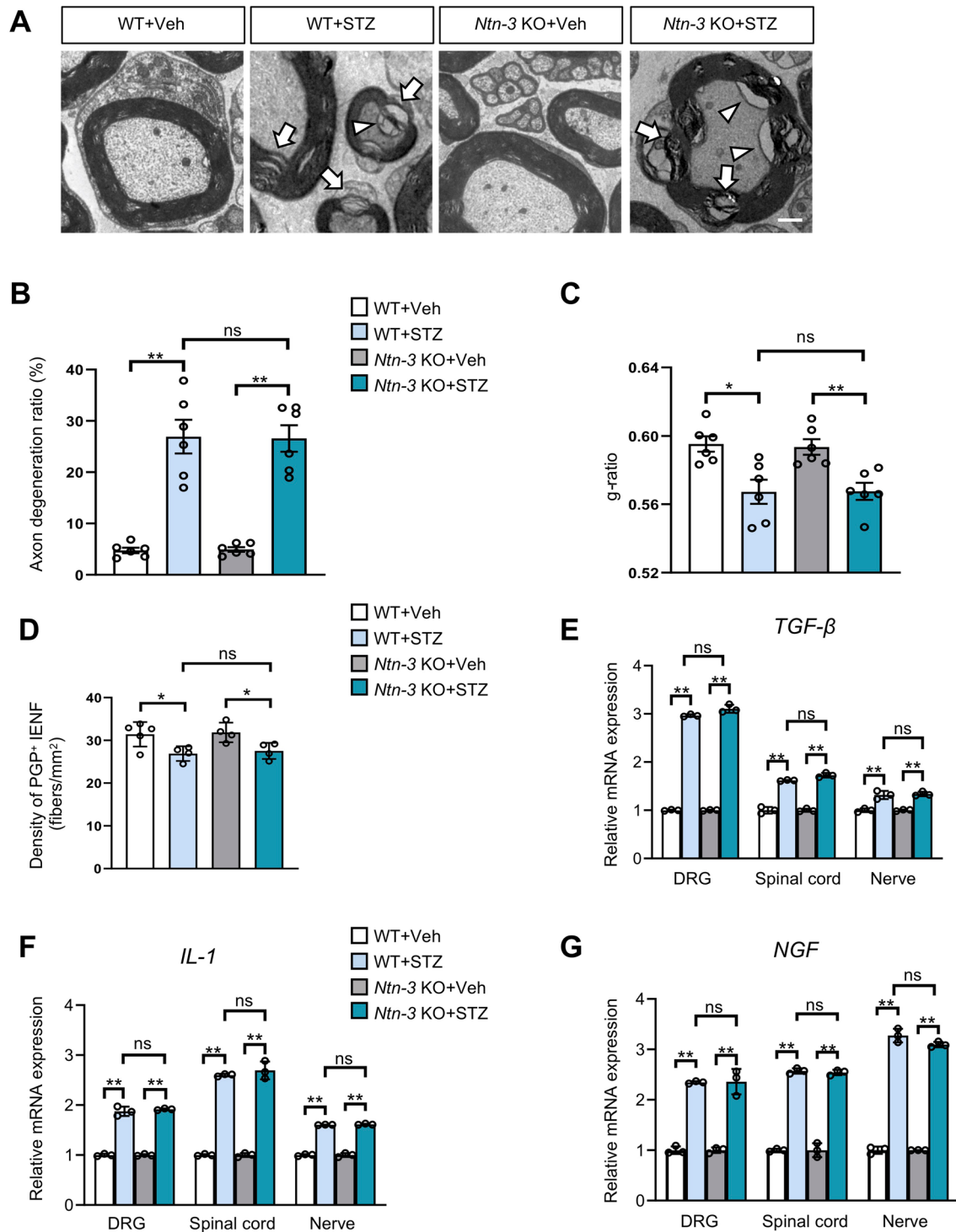


Fig. 3 *Ntn-3* deficiency does not affect peripheral nerve damage and neural inflammation. **A** Representative TEM images of sciatic nerves from vehicle- and STZ-treated WT and *Ntn-3* KO mice. Both demyelinating axons (arrows) and degenerating axons (arrowheads) are observed in STZ-induced diabetic mice. Scale bar, 1 μ m. **B** Axon degeneration in the sciatic nerve is evaluated by the axon degeneration ratio. **C** Demyelination of the sciatic nerve is evaluated by the g-ratio. **D** Quantification of PGP9.5⁺ intra-epidermal nerve fiber (IENF) density showing no significant difference in epidermal axon loss between diabetic WT and *Ntn-3* KO littermates. **E–G** QPCR analysis of *TGF- β* (E), *IL-1* (F), and *NGF* (G) expression in DRGs, spinal cords, and nerves from diabetic WT and *Ntn-3* KO mice.

** $P < 0.01$; ns, no significant difference by two-way ANOVA. $n = 6$ sections from 2 to 3 mice per group. **D** Quantification of PGP9.5⁺ intra-epidermal nerve fiber (IENF) density showing no significant difference in epidermal axon loss between diabetic WT and *Ntn-3* KO littermates. $*P < 0.05$; ns, no significant difference by two-way ANOVA. $n = 4–5$ mice per group. **E–G** QPCR analysis of *TGF- β* (E), *IL-1* (F), and *NGF* (G) expression in DRGs, spinal cords, and nerves from diabetic WT and *Ntn-3* KO mice. **E** *TGF- β* expression in DRG, spinal cord, and nerve. **F** *IL-1* expression in DRG, spinal cord, and nerve. **G** *NGF* expression in DRG, spinal cord, and nerve. ** $P < 0.01$; ns, no significant difference by two-way ANOVA. $n = 3$ mice per group.

significantly increased expression of these cytokines compared to their vehicle controls, while there was no difference between WT and *Ntn-3* KO animals regardless of STZ or vehicle treatment (Fig. 3E–G).

Ntn-3 Deficiency Facilitates the Intra-epidermal Sprouting of Sensory Axons

Previous studies have found that DNP is often associated with aberrant axon sprouting in epidermal areas [1, 3, 10, 11, 13, 14, 45, 46]. Therefore, we collected skin samples from the hind paws of diabetic WT and *Ntn-3* KO mice, in which the intra-epidermal sprouting of sensory axons was examined by immunostaining using the GAP-43 antibody. We found that few GAP-43⁺ axons were present in

the epidermis of both WT and *Ntn-3* KO mice after vehicle treatment, while the epidermal innervation of GAP-43⁺ axons was significantly increased after STZ administration with an even higher axon density in diabetic *Ntn-3* KO mice than diabetic WT mice (Fig. 4A, B). These data suggested that *Ntn-3* deficiency facilitates the intra-epidermal sprouting of sensory axons in diabetes.

To identify the sensory neuronal subtype of aberrant sprouting axons in *Ntn-3* KO mice, we conducted a retrograde labeling experiment by injecting Dil into the epidermal area of mouse hind paws. After 10 days, retrograde-labeled sensory neuron subtypes were determined by immunostaining with antibodies labeling the different subtypes. Interestingly, we found that most of the Dil-labeled neurons were CGRP⁺ sensory neurons in the DRGs of *Ntn-3* KO mice

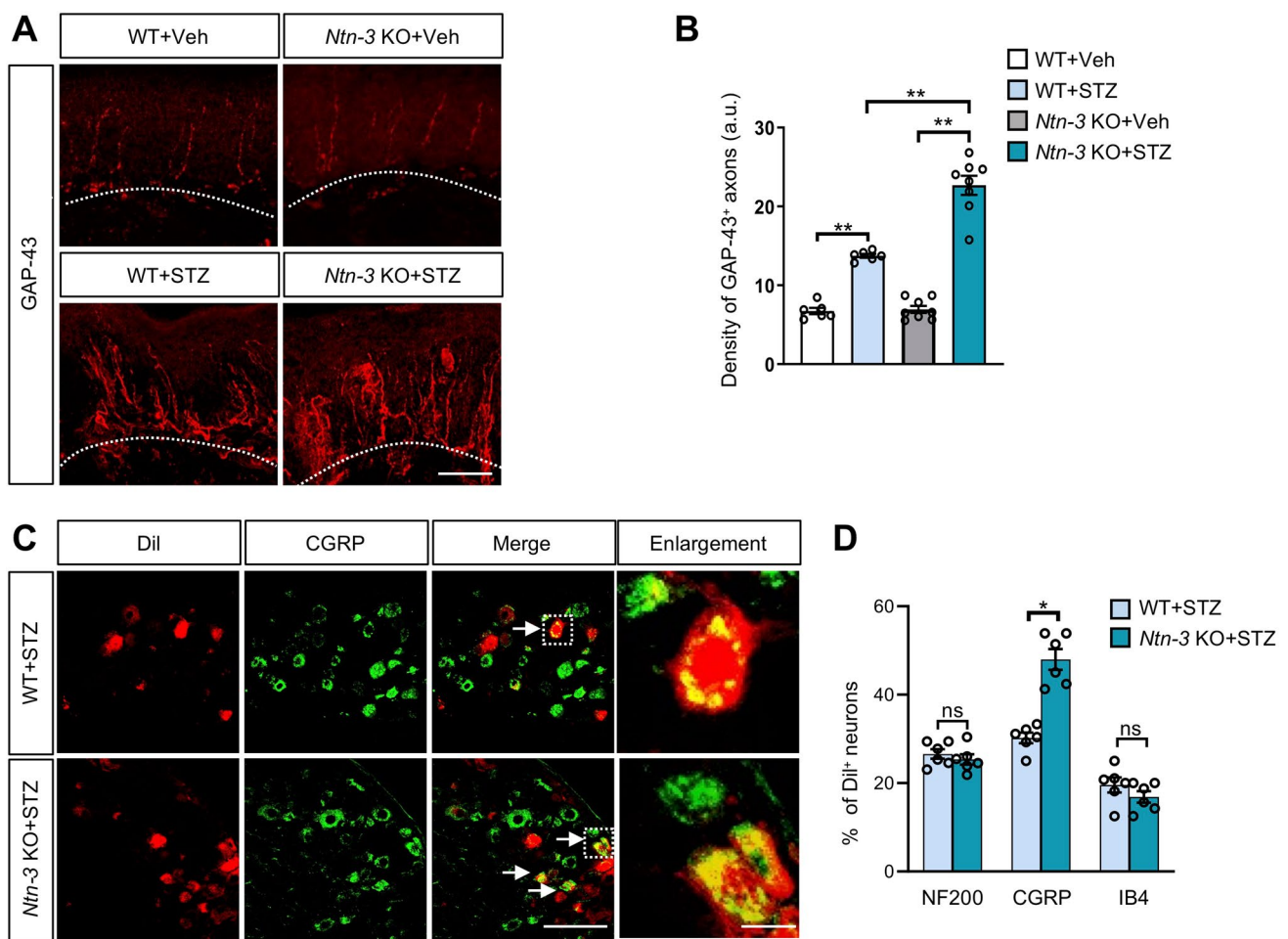


Fig. 4 *Ntn-3* deficiency causes the intra-epidermal sprouting of DRG sensory axons in diabetic mice. **A** Representative images of GAP-43 staining in hind paw skin samples were collected four weeks after STZ administration. Scale bar, 50 μ m. **B** Quantification of GAP-43 staining showing significantly increased axon sprouting in diabetic *Ntn-3* KO mice compared with diabetic WT mice. $**P < 0.01$ by two-way ANOVA. $n = 6$ –8 mice per group. **C** Representative images of CGRP and Dil double-labeled primary sensory neurons in the

DRGs of diabetic *Ntn-3* KO mice. Scale bar, 100 μ m. Boxed regions of the merged images are enlarged on the right. Scale bar, 15 μ m. **D** Percentages of NF200⁺, IB4⁺, CGRP⁺ neurons relative to Dil⁺ neurons in diabetic WT and *Ntn-3* KO mice. *Ntn-3* KO selectively facilitates the epidermal innervation of CGRP⁺ DRG neurons. $*P < 0.05$; ns, no significant difference by two-way ANOVA. $n = 6$ mice per group.

(Fig. 4C, D), indicating that Ntn-3 deficiency selectively promotes epidermal innervation by CGRP⁺ DRG neurons. These results were consistent with our finding that Ntn-3 was predominantly expressed in CGRP neurons (Fig. 1B, C).

Elevation of Ntn-3 Levels in DRGs Alleviates the Neuropathic Pain in Diabetic Mice

Along this line, we wondered whether the DNP could be relieved by elevating the Ntn-3 levels in DRGs. To assess this, we first delivered AAV-*Ntn-3* into mouse DRGs by i.t. injection (Fig. 5A). After 8 weeks, Ntn-3 expression was determined by qPCR analysis. We found that Ntn-3 expression exhibited a ~6-fold increase in DRGs infected with AAV-*Ntn-3* compared to AAV-*GFP*-infected controls (Fig. 5B). Moreover, by immunostaining, we found that AAV-*Ntn-3* was broadly expressed in DRG sensory neurons, especially in the CGRP⁺ subtype (Fig. S6).

Next, we injected these animals with STZ to induce hyperglycemia (Fig. 5A). By monitoring their blood glucose levels and body weight loss, we found that Ntn-3 overexpression did not affect the progression of hyperglycemia

(Fig. S7A, B). However, the von Frey test showed that the mechanical allodynia in AAV-*Ntn-3*-injected mice was significantly relieved to a level comparable to the non-diabetic mice (Fig. 5C). Similarly, their cold allodynia was also significantly alleviated (Fig. 5D).

The Intra-epidermal Sprouting of Sensory Axons is Suppressed by Ntn-3 Expression

To determine whether the DNP-associated axon sprouting is affected by Ntn-3 overexpression, we collected skin samples from the hind paws of AAV-*GFP* and AAV-*Ntn-3* infected mice 4 weeks after STZ or vehicle treatment. The intra-epidermal sprouting of sensory axons was examined by GAP-43 immunostaining. We found that the innervation of GAP-43⁺ axons was significantly lower in the epidermis of AAV-*Ntn-3*-infected diabetic mice than in AAV-*GFP*-infected diabetic mice, while AAV-*Ntn-3* treatment had no effect on the innervation of GAP-43⁺ axons in vehicle-treated control animals (Fig. 6A, B). These data highlighted the possibility that the pain-relieving effect of Ntn-3 is mediated by suppressing the intra-epidermal axon sprouting in diabetic mice.

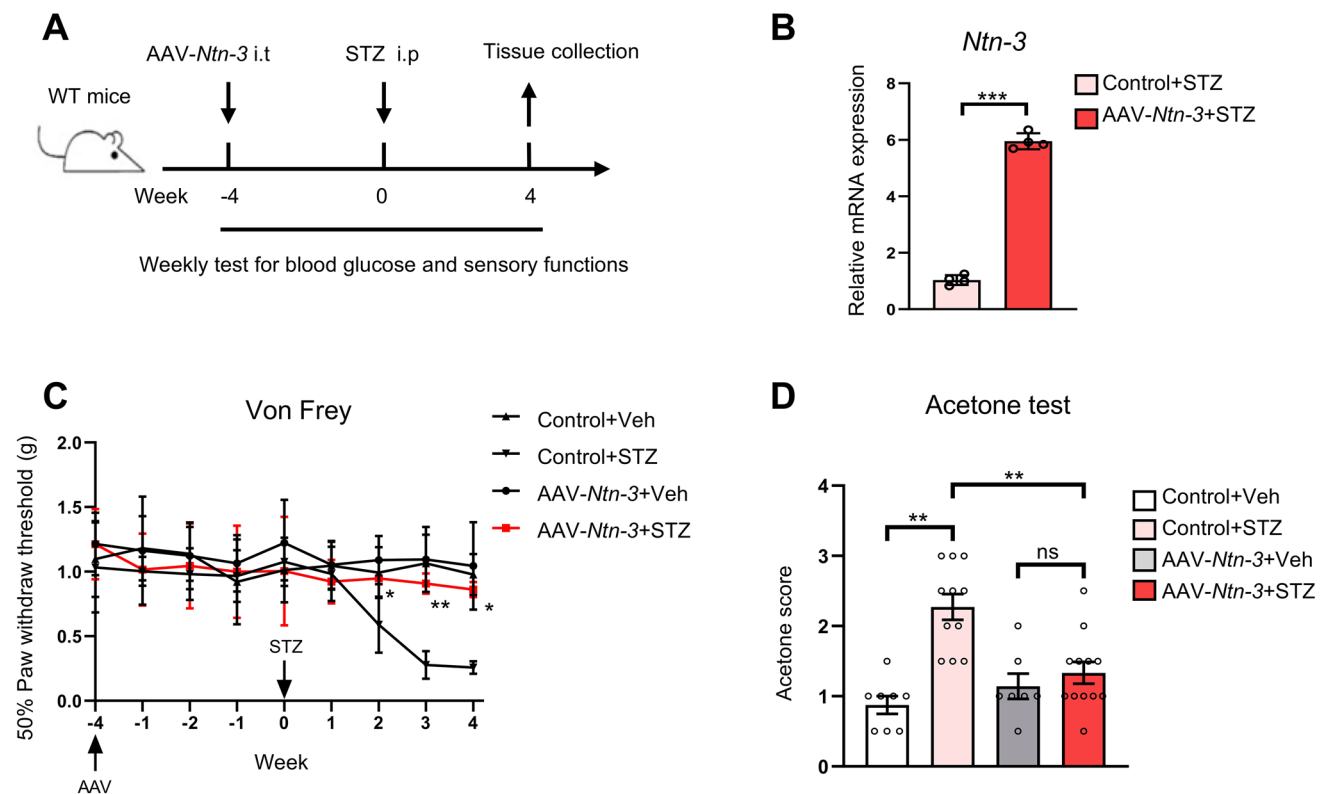


Fig. 5 Elevation of Ntn-3 expression in DRGs significantly alleviates DNP. **A** Schematic of the experimental design. **B** qPCR analysis showing *Ntn-3* expression is elevated in mouse DRGs by i.t. administration of AAV-*Ntn-3*. *** $P < 0.001$ by unpaired Student's *t*-test. $n = 4$ mice per group. **C** AAV-*Ntn-3* treatment significantly alleviates

mechanical allodynia in diabetic mice. * $P < 0.05$; ** $P < 0.01$ versus the Control+STZ group by two-way ANOVA. $n = 7$ –12 mice per group. **D** AAV-*Ntn-3* treatment significantly alleviates cold allodynia in diabetic mice. ** $P < 0.01$; ns, no significant difference by two-way ANOVA. $n = 7$ –12 mice per group.

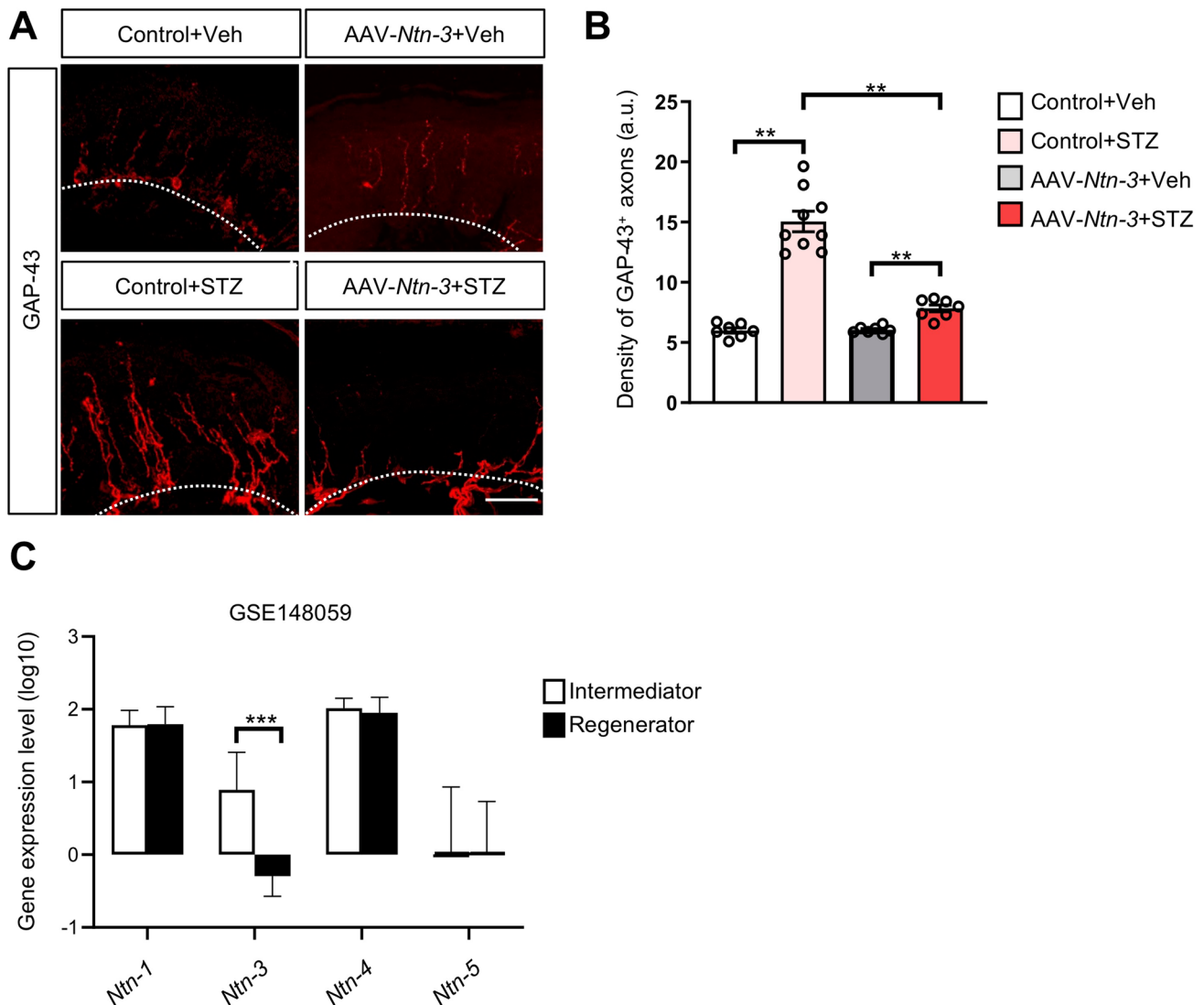


Fig. 6 Ntn-3 overexpression suppresses the intra-epidermal sprouting of sensory axons in diabetic mice. **A** Representative images of GAP-43 staining in mouse hind paw skin samples were collected four weeks after STZ administration. Scale bar, 50 μ m. **B** Quantification of GAP-43 staining showing significantly decreased axon sprouting

in diabetic mice after AAV-*Ntn-3* treatment. $**P < 0.01$ by two-way ANOVA. $n = 7-9$ mice per group. **C** Ntn-3 is significantly downregulated in diabetic neuropathy patients with more regenerating axons. $n \geq 14$ for diabetic neuropathy patients in each group. $***P < 0.001$ by unpaired Student's *t*-test.

Downregulation of Ntn-3 Expression is Correlated with the Regenerating Status of Peripheral Nerves in Diabetic Patients

Next, we wondered whether our findings in DNP mice are relevant to the clinical observations in diabetic patients with DNP. Since RNA-seq data have been generated from the sural nerve biopsies of diabetic patients in previous studies [41], we took advantage of this database to further analyze the correlation of Ntn-3 expression with DNP-associated pathological changes in that nerve in patients. Interestingly, our analysis showed that Ntn-3 was significantly downregulated in DNP patients with more regenerating axons,

suggesting that Ntn-3 expression is inversely correlated with the regeneration status of sural nerves in diabetic patients (Fig. 6C). However, other Ntn members were less relevant to this pathological event (Fig. 6C). These data supported our findings that Ntn-3 may be responsible for gating the aberrant sprouting of regenerating axons in diabetes.

Discussion

In the present work, we found that Ntn-3 was expressed in DRG sensory neurons, and downregulation of Ntn-3 expression was correlated with DNP severity in diabetic mice.

Ntn-3 deficiency stimulated the aberrant sprouting of sensory axons into epidermal areas, thus worsening the mechanical and cold allodynia in diabetic mice. In contrast, the elevation of Ntn-3 levels in DRGs alleviated the progression of DNP and suppressed the intra-epidermal sprouting of sensory axons. We also found that the downregulation of Ntn-3 expression was correlated with the regeneration status of peripheral nerves in diabetic patients.

The Contributions of Peripheral Nerve Pathology to DNP

The pathogenesis of diabetic neuropathy is often accompanied by two contradictory pathological changes in peripheral nerves: axon loss and regenerative axon sprouting. Because these two events occur simultaneously, their respective contributions to DNP remain indistinct. For example, the distal axon loss in the epidermal area has been used as the key morphological marker for the diagnosis of diabetic neuropathy [2, 4, 5, 33]; and inhibition of axon loss has been found to be beneficial for DNP treatment [34, 47]. On the other hand, there is evidence that the intra-epidermal sprouting of nerve fibers is strongly correlated with the development of DNP [1, 3, 10, 11, 13, 14, 45, 46], and inhibition of nerve fiber sprouting by anti-NGF treatment suppresses the mechanical allodynia in the mouse model of diabetic neuropathy [48]. Our findings here suggested that Ntn-3 may serve as a molecular probe, helping to dissect the contributions of these two nerve pathologies to the pathogenesis of DNP. Ntn-3 deficiency facilitated the aberrant intra-epidermal sprouting of sensory axons without affecting axon loss in diabetic animals. In this circumstance, *Ntn-3* KO mice still exhibited more severe DNP, suggesting that the axon loss is not essential for the development of DNP, and intra-epidermal sprouting of sensory axons is sufficient for inducing DNP, especially at the early stage of diabetic neuropathy.

The Function of Ntn-3 in Primary Sensory Neurons

Several studies have revealed that axon guidance molecules are not only implicated in neural wiring during development but also play important roles in axon regeneration and sprouting under pathological conditions [15–22]. As a functionally less-characterized Ntn family member, we found that Ntn-3 sustained its expression in DRG sensory neurons until adulthood. Genetic ablation of Ntn-3 did not cause any detectable developmental and behavioral defects in mice, probably due to functional compensations by other Ntn family members expressed in the nervous system [17–21]. However, Ntn-3 deficiency promoted the aberrant intra-epidermal sprouting of sensory axons in diabetes, contributing to increased DNP. Moreover, despite the fact that Ntn-3 expression is also found in neural tissues other than DRGs, i.e. injection-mediated

DRG-specific expression of Ntn-3 was sufficient to alleviate DNP progression by suppressing the intra-epidermal sprouting of sensory axons. Together, these results reveal an important fiber pathogenic function of Ntn-3 in sensory neurons. To the best of our knowledge, this study provides the first evidence for the function of Ntn-3.

In this study, there was an interesting finding that Ntn-3 depletion selectively worsens the mechanical and cold allodynia but not thermal pain in diabetic mice. Despite the underlying mechanism remaining unclear, it is worth noting that Ntn-3 is only expressed in a subpopulation of DRG sensory neurons. Therefore, one of the possible explanations is that Ntn-3 may only be expressed in the neuronal subtypes responsible for mechanical and cold allodynia but not for thermal hyperalgesia. Unfortunately, the present DRG neuronal subtype markers cannot precisely distinguish between them, but this is an interesting phenomenon to explore in the future.

Targeting the Ntn-3 Pathway for Developing the Treatment of Neuropathic Pain

DNP is one of the most common neuropathic pain conditions in the clinic and there is currently no cure. Our data highlight the possibility that Ntn-3 may serve as a druggable target for treating DNP. Along this line, future studies should be focused on identifying the receptors and downstream effectors of Ntn-3 signaling pathways, which may provide more molecular insights into the development of Ntn-3-based therapies. It is also important to explore whether Ntn-3 is implicated in other types of neuropathic pain given their similar pathological changes in peripheral nerves. Related studies may shed light on developing a uniform treatment for different types of neuropathic pain.

Acknowledgements We thank Dr. Naihe Jing (Shanghai Institute of Biochemistry and Cell Biology, Chinese Academy of Sciences) for discussing this project, and Beibei Wang (Center of Cryo-Electron Microscopy, Zhejiang University) for technical support. We are also grateful to Samuel L. Pfaff (The Salk Institute for Biological Studies) for providing reagents. This work was supported by the Zhejiang Provincial Natural Science Foundation of China (LY19H090030), the Science and Technology Innovation 2030-Major Project of Brain Science and Brain-like Research (2021ZD0202501), the Excellent Innovation Program of Hangzhou Municipal University in 2019, and the National Natural Science Foundation of China (82150003, 91949104, and 31871022).

Conflict of interest The authors declare that there are no conflicts of interest.

References

- Shillo P, Sloan G, Greig M, Hunt L, Selvarajah D, Elliott J. Painful and painless diabetic neuropathies: What is the difference? *Curr Diab Rep* 2019, 19: 32.

2. Feldman EL, Nave KA, Jensen TS, Bennett DLH. New horizons in diabetic neuropathy: Mechanisms, bioenergetics, and pain. *Neuron* 2017, 93: 1296–1313.
3. Themistocleous AC, Ramirez JD, Shillo PR, Lees JG, Selvarajah D, Orengo C, *et al.* The pain in neuropathy study (PiNS): A cross-sectional observational study determining the somatosensory phenotype of painful and painless diabetic neuropathy. *Pain* 2016, 157: 1132–1145.
4. Callaghan BC, Cheng HT, Stables CL, Smith AL, Feldman EL. Diabetic neuropathy: Clinical manifestations and current treatments. *Lancet Neurol* 2012, 11: 521–534.
5. Galer BS, Gianas A, Jensen MP. Painful diabetic polyneuropathy: Epidemiology, pain description, and quality of life. *Diabetes Res Clin Pract* 2000, 47: 123–128.
6. Alleman CJM, Westerhout KY, Hensen M, Chambers C, Stoker M, Long S, *et al.* Humanistic and economic burden of painful diabetic peripheral neuropathy in Europe: A review of the literature. *Diabetes Res Clin Pract* 2015, 109: 215–225.
7. Pop-Busui R, Boulton AJM, Feldman EL, Bril V, Freeman R, Malik RA, *et al.* Diabetic neuropathy: A position statement by the American diabetes association. *Diabetes Care* 2017, 40: 136–154.
8. Jensen TS, Backonja MM, Hernández Jiménez S, Tesfaye S, Valensi P, Ziegler D. New perspectives on the management of diabetic peripheral neuropathic pain. *Diab Vasc Dis Res* 2006, 3: 108–119.
9. Sloan G, Shillo P, Selvarajah D, Wu J, Wilkinson ID, Tracey I, *et al.* A new look at painful diabetic neuropathy. *Diabetes Res Clin Pract* 2018, 144: 177–191.
10. Cheng HT, Dauch JR, Porzio MT, Yanik BM, Hsieh W, Smith AG, *et al.* Increased axonal regeneration and swellings in intraepidermal nerve fibers characterize painful phenotypes of diabetic neuropathy. *J Pain* 2013, 14: 941–947.
11. Lauria G, Devigili G. Skin biopsy as a diagnostic tool in peripheral neuropathy. *Nat Clin Pract Neurol* 2007, 3: 546–557.
12. Bönhof GJ, Strom A, Püttgen S, Ringel B, Brüggemann J, Bódis K, *et al.* Patterns of cutaneous nerve fibre loss and regeneration in type 2 diabetes with painful and painless polyneuropathy. *Diabetologia* 2017, 60: 2495–2503.
13. Galosi E, la Cesa S, di Stefano G, Karlsson P, Fasolino A, Leone C, *et al.* A pain in the skin. Regenerating nerve sprouts are distinctly associated with ongoing burning pain in patients with diabetes. *Eur J Pain* 2018, 22: 1727–1734.
14. Üçeyler N, Vollert J, Broll B, Riediger N, Langjahr M, Saffer N, *et al.* Sensory profiles and skin innervation of patients with painful and painless neuropathies. *Pain* 2018, 159: 1867–1876.
15. Hollis ER 2nd. Axon guidance molecules and neural circuit remodeling after spinal cord injury. *Neurotherapeutics* 2016, 13: 360–369.
16. Domínguez-Romero ME, Slater PG. Unraveling axon guidance during axotomy and regeneration. *Int J Mol Sci* 2021, 22: 8344.
17. Brignani S, Raj DDA, Schmidt ERE, Düdükçü Ö, Adolfs Y, de Ruiter AA, *et al.* Remotely produced and axon-derived netrin-1 instructs GABAergic neuron migration and dopaminergic substantia nigra development. *Neuron* 2020, 107: 684–702.e9.
18. Dominici C, Moreno-Bravo JA, Puiggros SR, Rappeneau Q, Rama N, Vieugue P, *et al.* Floor-plate-derived netrin-1 is dispensable for commissural axon guidance. *Nature* 2017, 545: 350–354.
19. Goldman JS, Ashour MA, Magdesian MH, Tritsch NX, Harris SN, Christofi N, *et al.* Netrin-1 promotes excitatory synaptogenesis between cortical neurons by initiating synapse assembly. *J Neurosci* 2013, 33: 17278–17289.
20. Chen GQ, Kang SS, Wang ZH, Ahn EH, Xia YY, Liu X, *et al.* Netrin-1 receptor UNC5C cleavage by active δ -secretase enhances neurodegeneration, promoting Alzheimer's disease pathologies. *Sci Adv* 2021, 7: eabe4499.
21. Lin L, Lesnick TG, Maraganore DM, Isacson O. Axon guidance and synaptic maintenance: Preclinical markers for neurodegenerative disease and therapeutics. *Trends Neurosci* 2009, 32: 142–149.
22. Rajasekharan S, Kennedy TE. The netrin protein family. *Genome Biol* 2009, 10: 239.
23. Wang H, Copeland NG, Gilbert DJ, Jenkins NA, Tessier-Lavigne M. Netrin-3, a mouse homolog of human NTN2L, is highly expressed in sensory ganglia and shows differential binding to netrin receptors. *J Neurosci* 1999, 19: 4938–4947.
24. Sun C, Zhang F, Ge XJ, Yan TT, Chen XM, Shi XL, *et al.* SIRT1 improves insulin sensitivity under insulin-resistant conditions by repressing PTP1B. *Cell Metab* 2007, 6: 307–319.
25. Jolivald CG, Frizzi KE, Guernsey L, Marquez A, Ochoa J, Rodriguez M, *et al.* Peripheral neuropathy in mouse models of diabetes. *Curr Protoc Mouse Biol* 2016, 6: 223–255.
26. Kraeuter AK, Guest PC, Sarnyai Z. The open field test for measuring locomotor activity and anxiety-like behavior. *Methods Mol Biol* 2019, 1916: 99–103.
27. Chadman KK, Gong S, Scattoni ML, Boltuck SE, Gandhi SU, Heintz N, *et al.* Minimal aberrant behavioral phenotypes of neurexophilin-3 R451C knockin mice. *Autism Res* 2008, 1: 147–158.
28. He WW, Bai G, Zhou HH, Wei N, White NM, Lauer J, *et al.* CMT2D neuropathy is linked to the neomorphic binding activity of glycyl-tRNA synthetase. *Nature* 2015, 526: 710–714.
29. Wang GH, Jiang XY, Pu HJ, Zhang WT, An CR, Hu XM, *et al.* Scriptaid, a novel histone deacetylase inhibitor, protects against traumatic brain injury via modulation of PTEN and AKT pathway: Scriptaid protects against TBI via AKT. *Neurotherapeutics* 2013, 10: 124–142.
30. Chaplan SR, Bach FW, Pogrel JW, Chung JM, Yaksh TL. Quantitative assessment of tactile allodynia in the rat paw. *J Neurosci Methods* 1994, 53: 55–63.
31. de la Calle JL, Mena MA, González-Escalada JR, Paíno CL. Intrathecal transplantation of neuroblastoma cells decreases heat hyperalgesia and cold allodynia in a rat model of neuropathic pain. *Brain Res Bull* 2002, 59: 205–211.
32. Manering NA, Reuter T, Ihmsen H, Yeomans DC, Tzabazis A. High-dose remifentanyl prevents development of thermal hyperalgesia in a neuropathic pain model. *Br J Anaesth* 2013, 110: 287–292.
33. Zhu SA, Zhu JX, Zhen GH, Hu YH, An SB, Li YS, *et al.* Subchondral bone osteoclasts induce sensory innervation and osteoarthritis pain. *J Clin Invest* 2019, 129: 1076–1093.
34. Cheng YL, Liu J, Luan Y, Liu ZY, Lai HJ, Zhong WL, *et al.* Sarm1 gene deficiency attenuates diabetic peripheral neuropathy in mice. *Diabetes* 2019, 68: 2120–2130.
35. Poitras T, Chandrasekhar A, McCoy L, Komirishetty P, Areti A, Webber CA, *et al.* Selective sensory axon reinnervation and TRPV1 activation. *Mol Neurobiol* 2019, 56: 7144–7158.
36. Liu HQ, Dolkas J, Hoang K, Angert M, Chernov AV, Remacle AG, *et al.* The alternatively spliced fibronectin CS1 isoform regulates IL-17A levels and mechanical allodynia after peripheral nerve injury. *J Neuroinflammation* 2015, 12: 158.
37. Choi J, Kim DS, Kim J, Jeong W, Lee HW, Park SW, *et al.* Better nerve regeneration with distally based fascicular turnover flap than with conventional autologous nerve graft in a rat sciatic nerve defect model. *J Plast Reconstr Aesthet Surg* 2020, 73: 214–221.
38. Beirowski B, Babetto E, Golden JP, Chen YJ, Yang K, Gross RW, *et al.* Metabolic regulator LKB1 is crucial for Schwann cell-mediated axon maintenance. *Nat Neurosci* 2014, 17: 1351–1361.
39. Hylden JL, Wilcox GL. Intrathecal morphine in mice: A new technique. *Eur J Pharmacol* 1980, 67: 313–316.
40. Chen G, Xie RG, Gao YJ, Xu ZZ, Zhao LX, Bang SS, *et al.* β -arrestin-2 regulates NMDA receptor function in spinal lamina II neurons and duration of persistent pain. *Nat Commun* 2016, 7: 12531.

41. Guo K, Eid SA, Elzinga SE, Pacut C, Feldman EL, Hur J. Genome-wide profiling of DNA methylation and gene expression identifies candidate genes for human diabetic neuropathy. *Clin Epigenetics* 2020, 12: 123.
42. Hur J, Sullivan KA, Callaghan BC, Pop-Busui R, Feldman EL. Identification of factors associated with sural nerve regeneration and degeneration in diabetic neuropathy. *Diabetes Care* 2013, 36: 4043–4049.
43. Løseth S, Stålberg E, Jorde R, Mellgren SI. Early diabetic neuropathy: Thermal thresholds and intraepidermal nerve fibre density in patients with normal nerve conduction studies. *J Neurol* 2008, 255: 1197–1202.
44. Zhou JY, Zhou SW. Inflammation: therapeutic targets for diabetic neuropathy. *Mol Neurobiol* 2014, 49: 536–546.
45. Anand P, Bley K. Topical capsaicin for pain management: Therapeutic potential and mechanisms of action of the new high-concentration capsaicin 8% patch. *Br J Anaesth* 2011, 107: 490–502.
46. Yoo M, Sharma N, Pasnoor M, Kluding PM. Painful diabetic peripheral neuropathy: Presentations, mechanisms, and exercise therapy. *J Diabetes Metab* 2013, Suppl 10: 005.
47. Singh B, Singh V, Krishnan A, Koshy K, Martinez JA, Cheng C, *et al.* Regeneration of diabetic axons is enhanced by selective knockdown of the PTEN gene. *Brain* 2014, 137: 1051–1067.
48. Cheng HT, Dauch JR, Hayes JM, Yanik BM, Feldman EL. Nerve growth factor/p38 signaling increases intraepidermal nerve fiber densities in painful neuropathy of type 2 diabetes. *Neurobiol Dis* 2012, 45: 280–287.

Springer Nature or its licensor (e.g. a society or other partner) holds exclusive rights to this article under a publishing agreement with the author(s) or other rightsholder(s); author self-archiving of the accepted manuscript version of this article is solely governed by the terms of such publishing agreement and applicable law.